2442 *Chem. Mater.* **2010,** *22,* 2442–2450
DOI:10.1021/cm903785r

CHEMISTRY OF MATERIALS
Article

New Strategy to Synthesis of Hierarchical Mesoporous Zeolites

Fang Na Gu,[†,‡] Feng Wei,[†] Jia Yuan Yang,[†] Na Lin,[†] Wei Gang Lin,[†] Ying Wang,[‡] and Jian Hua Zhu*,[†]

[†]*Key Laboratory of Mesoscopic Chemistry of MOE, College of Chemistry and Chemistry Engineering, Nanjing University, Nanjing 210093, China, and* [‡]*Ecomaterials and Renewable Energy Research Center (ERERC), Nanjing University, Nanjing 210093, China.*

Received July 11, 2009. Revised Manuscript Received March 3, 2010

We report a new strategy to synthesize the hierarchical mesoporous zeolite through design of mesoscale cationic surfactant cetyltrimethylammonium bromide (CTAB) micelle with cosolvent tert-butyl alcohol (TBA) and the 1,3,5-trimethylbenzene (TMB) additive, by which the formation of hierarchical mesostructure arose from the condensing of zeolite fragments on the mesoscale surfactant micelles. The hierarchical mesoporous silica with zeolite Y or sodalite fragment is synthesized for the first time, which exhibited both the mesostructure and the typical diffraction of zeolite. XRD, N_2 adsorption−desorption, ^{27}Al MAS NMR, FTIR, and NH_3-TPD techniques were employed to characterize the resulting samples, and the adsorption of NPYR (*N*-nitrosopyrrolidine) and NNN (*N*-nitrosonornicotine) were performed to assess the adsorptive capability of the zeolitic mesoporous materials. The MS3-4t-5b sample synthesized by assembling zeolite gel exhibited the adsorptive capacity comparable to NaY zeolite for trapping NPYR in airflow but four times superior to NaY for adsorbing bulky nitrosamine NNN in solution because of its hierarchical mesostructure.

1. Introduction

Crystals of zeolites with unique properties, such as high-surface area, acidity, and shape selectivity characters, have been widely used in industry as heterogeneous catalysts, especially as the solid acid catalysts in the fields of oil refining and petrochemistry.[1] However, the sole presence of micropores in zeolites often imposes diffusion limitations because of the restricted access and slow intracrystalline transport to and from the active site,[2,3] provoking the low catalytic efficiency. To overcome this problem, various strategies such as the synthesis of nanosized zeolites,[4] ultralarge-pore zeolites,[5] and zeolite analogues have been adopted.[6] Nevertheless, the application of these materials is fairly limited because of the difficult separation of nanosized zeolite crystals from the reaction mixture and the complexity of the templates used for the synthesis of ultra-large-pore zeolites.

The new mesoporous and micropores composite that combine both the pore structure advantage of mesopore and the strong acidity of zeolite, is one of the most promising materials with fast diffusive rate, and many exposed active sites. And the method widely employed to generate mesopore involves the leaching treatments of zeolite crystals by acid or alkali,[7,8] dry-gel conversion to transform the amorphous mesoporous silica into zeolite[9−11] and hard-template-directed synthesis.[12−16] However, the mesopores generated by the extraction of aluminum or silicon from the zeolite lattice were predominantly isolated, resulting in the insignificantly enhanced intracrystalline diffusion. Although the CMK templating method could establish an ordered mesoporous aluminosilicate with a complete crystalline zeolite wall structure and a narrow pore size distribution,[13] the complicated preparation of CMK template limited its industrial application.

In light of the success in the preparation of ordered mesoporous materials from the self-assembly of small silica species with various surfactants,[17,18] a mixed-template

*To whom correspondence should be addressed. E-mail: jhzhu@netra.nju.edu.cn. Phone: 86-25-83595848. Fax: 86-25-83317761.

(1) Davis, M. E. *Nature* **2002**, *417*, 813.
(2) Hartmann, M. *Angew. Chem., Int. Ed.* **2004**, *43*, 5880.
(3) Pérez-Ramírez, J.; Christensen, C. H.; Egeblad, K.; Christensen, C. H.; Groen, J. C. *Chem. Soc. Rev.* **2008**, *37*, 2530.
(4) Tosheva, L.; Valtchev, V. P. *Chem. Mater.* **2005**, *17*, 2494.
(5) Corma, A.; Díaz-Cabañas, M. J.; Jordá, J. L.; Martínez, C.; Moliner, M. *Nature* **2006**, *443*, 842.
(6) Strohmaier, K. G.; Vaughan, D. W. *J. Am. Chem. Soc.* **2003**, *125*, 16035.
(7) Groen, J. C.; Peffer, L. A. A.; Moulijn, J. A.; Pérez-Ramírez, J. *Chem.—Eur. J.* **2005**, *11*, 4983.
(8) Pérez-Ramírez, J.; Abelló, S.; Bonilla, A.; Groen, J. C. *Adv. Funct. Mater.* **2009**, *19*, 164.
(9) Yue, M. B.; Sun, L. B.; Zhuang, T. T.; Dong, X.; Chun, Y.; Zhu, J. H. *J. Mater. Chem.* **2008**, *18*, 2044.
(10) Campos, A. A.; Dimitrov, L.; da Silva, C. R.; Wallau, M.; Urquieta-González, E. A. *Microporous Mesoporous Mater.* **2006**, *95*, 92.
(11) Trong, On, D.; Kaliaguine, S. *Angew. Chem., Int. Ed.* **2001**, *40*, 3248.
(12) Yang, Z.; Xia, Y.; Mokaya, R. *Adv. Mater.* **2004**, *16*, 727.
(13) Fang, Y.; Hu, H. *J. Am. Chem. Soc.* **2006**, *128*, 10636.
(14) Jacobsen, C. J. H.; Madsen, C.; Houzvicka, J.; Schmidt, I.; Carlsson, A. *J. Am. Chem. Soc.* **2000**, *122*, 7116.
(15) Tao, Y. S.; Kanoh, H.; Kaneko, K. *J. Am. Chem. Soc.* **2003**, *125*, 6044.
(16) Zhu, H. B.; Liu, Z. C.; Wang, Y. D.; Kong, D. J.; Yuan, X. H.; Xie, Z. K. *Chem. Mater.* **2008**, *20*, 1134.
(17) Kresge, C. T.; Leonowicz, M. E.; Roth, W. J.; Vartuli, J. C.; Beck, J. S. *Nature* **1992**, *359*, 710.

 Published on Web 03/23/2010

synthesis approach was introduced.[19,20] An early attempt to prepare a mesoporous zeolite material via dual templating, that is, using both molecular and supramolecular templates in a one-step synthesis, was based on the idea that the molecular templates could direct zeolite crystallization in the mesopore walls, while the mesoporous structure was simultaneously formed according to the supramolecular templating mechanism of the surfactant micelles. In fact, however, the two templating system worked in a competitive, rather than cooperative manner, which resulted in the formation of the bulk zeolite without any mesoporosity, the amorphous mesoporous material, or their physical mixtures.[20] To solve the phase-separation problem, amphiphilic organosilanes[21,22] or silane-founctionalized polymers[23] were introduced into the silica−alumina sol−gel reaction mixture as the mesopore-directing agents, because the hydrolyzable methoxysilyl moiety, contained in the surfactant, could strongly interact with the growing crystal domains through the formation of covalent bonds with other SiO_2 and Al_2O_3 sources to avoid phase separation. The resulting materials exhibited the interconnected mesopores with zeolitic pore walls, but their mesoporous volumes were relative small. Besides using these unavailable hydrolyzable methoxysilyl moiety containing surfactants by one-pot method, the crystal surfactant-mediated assembly of zeolite seeds into mesoporous structures emerged as a promising alternative.[24−27] This approach is based on two steps, the first step of synthesizing the proto-zeolitic nanoclusters (known as zeolite seeds), and the second step of assembling these zeolite seed crystals into mesoporous structure under the directing of surfactant. The obtained products exhibited an ordered mesoporous structure,[24,25] but no the typical X-ray diffraction (XRD) peak of zeolites, because these materials did not have the long-range atomic order characteristic of a crystalline zeolite framework because of the relatively small size of preformed zeolite nanoclusters (less than several nanometers). As a result, the properties of these final materials were still far from those of crystalline zeolites, which make them insufficient for many industrial applications.[27] To obtain the materials with intact zeolite unit, the crystal sizes of zeolite seeds should be larger than 5 nm;[27] however, in this case, it is not easy to take a self-assembly between bulky silica species with the surfactants because of the lack of strong interaction between the bulky silica species and the current surfactants that have a limited charge density.[28]

Reviewing the research reported in literature,[29,30] a new strategy is proposed here to conquer the difficulty abovementioned: adding the cosolvent to alter the assembly of surfactant micelle and increase the charge density of the micelle, enhancing the interaction toward the silica species; Simultaneously, TMB is used to swell the surfactant micelle to mesoscale so that the micelle can match the zeolitic silicate species in size. Moreover, the introduction of TMB could accelerate the structuring of surfactant aggregates and the polymerization of solid.[31] Herein, we report an alternative and simple route for the synthesis of the stable zeolitic mesoporous materials with high surface area and large pore volume from the self-assembly of zeolite nanocrystals with CTAB surfactant and cosolvent, as well as the TMB agent, in which TMB enlarges the geometrical dimension of surfactant micelle, while the cosolvent strengthens the charge density of micelle, enabling the surfactants to exert the directing function toward zeolite fragments. Apart from the characterization of these hierarchical mesoporous zeolites with the techniques of XRD, N_2 adsorption−desorption, ^{27}Al MAS NMR, FTIR, and NH_3-TPD, the actual performance of theses materials are assessed by the adsorption of the volatile nitrosamine NPYR and bulky nitrosamine NNN, to expand their potential application in the protection of environment.

2. Experimental Section

NPYR and NNN were purchased from Sigma and dissolved in dichloromethane (A.R.) respectively at the ratio of 1:19 (v/v). Tetraethylorthosilicate (TEOS) and cetyltrimethylammonium bromide (CTAB) were the products of Shanghai Wulian and Lingfeng Companies (China), and other regents with the A.R. purity were used as received. NaY was the commercially available powder with the Si/Al ratio of 2.86. AM10 and AM3 was the normal Al-containing MCM-41 with Si/Al of 10 or 3 synthesized according to literature.[32]

2.1. Synthesis of Samples. To synthesize the hierarchical mesoporous composite with type Y zeolite unit, sodium silicate and sodium aluminate were used as the silica and aluminum source, respectively. Sodium silicate (5.68 g) was dissolved in 11.3 g of distilled water, followed by adding a solution of 0.16 g sodium aluminate in 8 g tetramethylammonium hydroxide (TMAOH, 25 wt % aqueous solution). The resulting solution was stirred at room temperature for 30 min and then hydrothermally treated at 130 °C for 72 h. After the colloidal product was cooled to room temperature, a solution of 1.7 g CTAB, a calculated amount of 1,3,5-trimethylbenzene (TMB) and cosolvent *tert*-butyl alcohol (TBA) in 12 g of distilled water were

(18) Zhao, D.; Feng, J.; Huo, Q.; Melosh, N.; Fredrickson, G. H.; Chmelka, B. F.; Stucky, G. D. *Science* **1998**, *279*, 548.
(19) Karlsson, A.; Stocker, M.; Schmidt, R. *Microporous Mesoporous Mater.* **1999**, *27*, 181.
(20) Petkov, N.; Holzl, M.; Metzger, T. H.; Mintova, S.; Bein, T. *J. Phys. Chem. B* **2005**, *109*, 4485.
(21) Choi, M.; Cho, H. S.; Srivastava, R.; Venkatesan, C.; Choi, D.-H.; Ryoo, R. *Nat. Mater.* **2006**, *5*, 718.
(22) Choi1, M.; Na, K.; Kim, J.; Sakamoto, Y.; Terasaki, O.; Ryoo, R. *Nature* **2009**, *461*, 246.
(23) Wang, H.; Pinnavaia, T. J. *Angew. Chem., Int. Ed.* **2006**, *45*, 7603.
(24) Liu, Y.; Zhang, W.; Pinnavaia, T. J. *J. Am. Chem. Soc.* **2000**, *122*, 8791.
(25) Tong, On, D.; Kaliaguine, S. *J. Am. Chem. Soc.* **2003**, *125*, 618.
(26) Zhang, Z.; Han, Y.; Zhu, L.; Wang, R.; Yu, Y.; Qiu, S.; Zhao, D.; Xiao, F.-S. *Angew. Chem., Int. Ed.* **2001**, *40*, 1258.
(27) Xia, Y.; Mokaya, R. *J. Mater. Chem.* **2004**, *14*, 3427.
(28) Song, J. W.; Ren, L. M.; Yin, C. Y.; Ji, Y. Y.; Wu, Z. F.; Li, J. X.; Xiao, F. -S. *J. Phys. Chem. C* **2008**, *112*, 8609.
(29) Flodström, K.; Wennerström, H.; Alfredsson, V. *Langmuir* **2004**, *20*, 680.
(30) Xiao, F.-S.; Wang, L. F.; Yin, C. Y.; Lin, K. F.; Di, Y.; Li, J. X.; Xu, R. R.; Su, D. S; Schlögl, R.; Yokoi, T.; Tatsumi, T. *Angew. Chem., Int. Ed.* **2006**, *45*, 3090.
(31) Ottaviani, M. F.; Moscatelli, A.; Desplantier-Giscard, D.; Di Renzo, F.; Kooyman, P. J.; Alonso, B.; Galarneau, A. *J. Phys. Chem. B* **2004**, *108*, 12123.
(32) Gu, F. N.; Zhou, Y.; Wei, F.; Wang, Y.; Zhu, J. H. *Microporous Mesoporous Mater.* **2009**, *126*, 143.

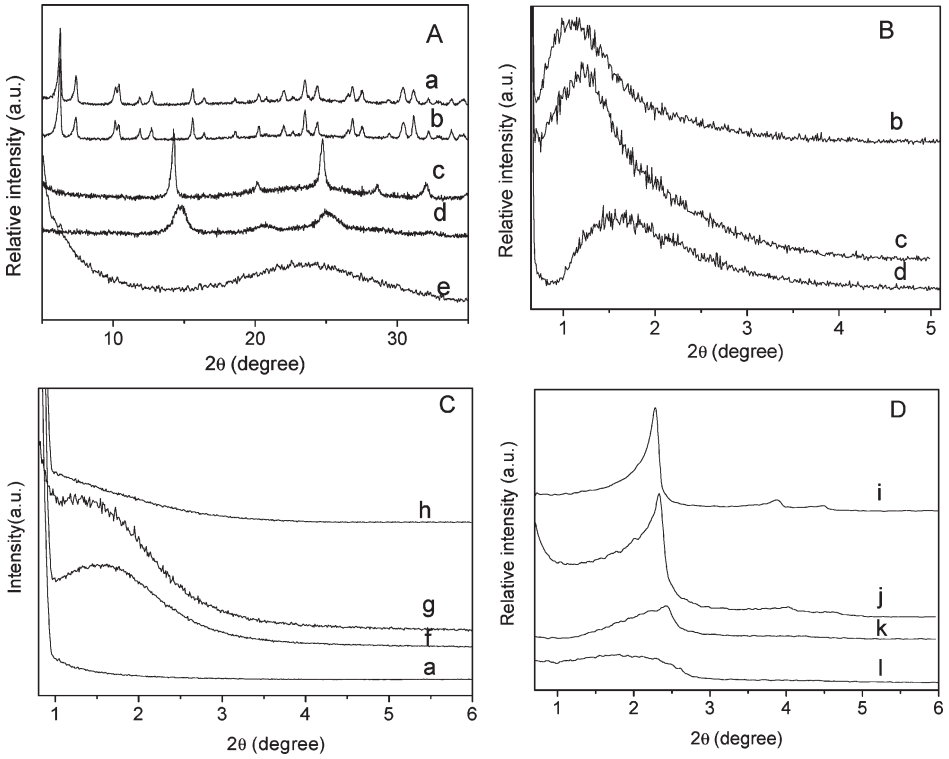

Figure 1. (A) Wide-angle and (B) low-angle XRD patterns of (a) MS3, (b) MS3-4t-5b, (c) MT3-4t-5b, (d) MT10-4t-5b, and (e) AM10. (C) Low-angle XRD patterns of MS samples synthesized with different amounts of TMB or TBA: (a) MS3, (f) MS3-4t-7b, (g) MS3-6t-5b, and (h) MS3-9t-5b. (D) Low-angle XRD patterns of MT10 (i, j) and the normal AM10 (k, l) samples before (i, k) and after (j, l) the hydrothermal treatment.

added dropwise into the colloidal product, and then the pH value of the synthetic system was adjusted to 10 with HCl. The obtained mixture was stirred at room temperature for 1 h. After it was aged at 100 °C for 24 h, the solid product was collected by filtrating, drying, and calcination at 550 °C for 5 h. For comparison, TEOS was used as silica source instead of sodium silicate, while other conditions were kept as the same. The final obtained samples were labeled as MS*x*-*y*t-*z*b or MT*x*-*y*t-*z*b, where S and T meant sodium silicate and TEOS, respectively, *x* indicated the molar ratio of silicon to aluminum in the initial gel, *y* was the molar ratio of TMB (t) to CTAB, and *z* was the mass of the added TBA (b).

2.2. Characterization. To characterize the sample in detail, the XRD patterns were recorded on an ARL XTRA diffractometer with Cu K_α radiation in the 2θ range of 0.5−6° or 5−70°. FTIR spectrum was recorded on a Bruker 22 infrared spectrophotometer in 4000−400 cm^{-1} with a resolution of 4 cm^{-1} using KBr pellet containing 3-wt.% of sample. Nitrogen adsorption isotherms were measured at −196 °C on a Micromeritics ASAP 2020 volumetric adsorption analyzer, and the sample was outgassed at 300 °C for 4 h prior to test. The BET specific surface area of sample was calculated using adsorption data acquired at a relative pressure (p/p_0) range of 0.05−0.22, and the total pore volume was determined from the amount adsorbed at the relative pressure of about 0.99. Pore size distributions (PSD) were evaluated from the adsorption isotherms by the Density Functional Theory method,[33] and the microporous volume was evaluated by the *t*-plot method.[34,35] To assess the hydrothermal stability of the hierarchical mesoporous zeolites, the MT sample and the normal Al-MCM-41 with similar aluminum content were refluxed with the boiling water of 100 $mL \cdot g^{-1}$ for 12 h and then examined by XRD test. To check the influence of coke on the adsorption of normal zeolite NaY and mesoporous zeolite NaY, the samples were treated with benzene (0.75 $mL \cdot g^{-1}$) at 500 °C in the flow of nitrogen (99.99%). The carbon content of NaY zeolite after coking was analyzed by Heraeus CHN−O-Rapid Element Analyzer.

The experiment of ^{27}Al MAS NMR, temperature programmed desorption (TPD) of ammonia,[32] the catalytic decomposition of 2-propanol, liquid adsorptions of NNN, and the instantaneous adsorption of NPYR were carried out in the process reported previously.[36−38]

3. Results

Figure 1A shows the wide-angle XRD patterns of various MS samples synthesized by using sodium silicate as silica source and the molar Si/Al ratio of the zeolite gel was 3. All of the MS samples exhibited the typical diffraction peaks of zeolite Y,[39] indicating the formation of intact zeolite cells. In the presence of swell agent TMB and cosolvent TBA, the resulting sample MS3−4t-5b exhibited

(33) Ridha, F. N.; Yang, Y. X.; Webley, P. A. *Microporous Mesoporous Mater.* **2009**, *117*, 497.
(34) Tang, Q. H.; Zhang, Q. H.; Wang, P; Wang, Y.; Wan, H. L. *Chem. Mater.* **2004**, *16*, 1967–1976.
(35) (a) Kruk, M.; Jaroniec, M.; Ko, C. H.; Ryoo, R. *Chem. Mater.* **2000**, *12*, 1961. (b) Jaroniec, M.; Kruk, M.; Olivier, J. P. *Langmuir* **1999**, *15*, 5410.
(36) Cao, Y.; Shi, L. Y.; Zhou, C. F.; Yun, Z. Y.; Wang, Y.; Zhu, J. H. *Environ. Sci. Technol.* **2005**, *39*, 7254.
(37) Sun, L. B.; Gu, F. N.; Chun, Y.; Kou, J. H.; Yang, J.; Wang, Y.; Zhu, J. H.; Zou, Z. G. *Microporous Mesoporous Mater.* **2008**, *116*, 498.
(38) Zhou, C. F.; Cao, Y.; Zhuang, T. T.; Huang, W.; Zhu, J. H. *J. Phys. Chem. C.* **2007**, *111*, 4347.
(39) Tao, Y. S.; Kanoh, H.; Kaneko, K. *J. Phys. Chem. B* **2003**, *107*, 10974.

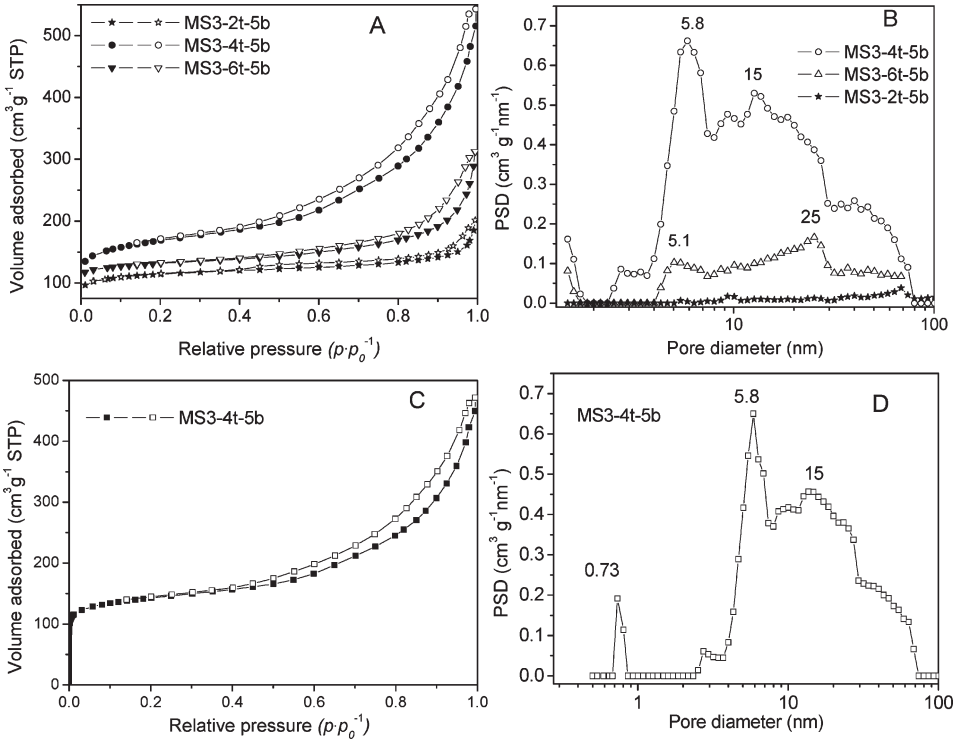

Figure 2. Nitrogen adsorption−desorption isotherms (A, C) and pore distribution curves (B, D) of porous samples.

a broad peak in its low-angle XRD patterns (Figure 1B), mirroring the formation of a worm-like mesoporous phase.[40] As the amount of TMB increased, the diffraction peak of MS3-6t-5b sample shifted to the low-angle slightly and the peak intensity decreased since a emulsion analog formed. When the molar ratio of TMB to CTAB was up to 9, mesostructure was absent in the synthesized MS3-9t-5b sample (Figure 1C). However, without or introduction of a small quantity of TMB into the reaction system, the resulting product MS3 and MS3-2t-5b showed no mesostructure, either (Figure 1C). Similarly, the amount of TBA additive was also crucial in this synthesis; once the amount of TBA decreased to 2 g, the precipitation emerged in the mixture of CTAB and TMB, and mesostructure was absent in the final product MS3-4t-2b. Fortunately, the adjusting was feasible in a narrow range, and the resulting MS3−4t-7b sample exhibited the mesostructure similar to MS3-4t-5b (Figure S1, Supporting Information).

When TEOS was used as the silica source, while other synthesis conditions were the same as that of MS-4t-5b, the obtained MT3-4t-5b sample also possessed a worm-like mesoporous phase (profile c in Figure 1B), but the diffraction peaks in its wide-angle XRD patterns were attributed to sodalite instead of zeolite Y (profile c in Figure 1A),[41] implying that tuning the silica source can result in the mesoporous zeolite with different crystalline type. However, disordered products were obtained once TMB and TBA were absent (low-angle XRD patterns not shown), and this phenomenon mirrored the important role played by TMB and cosolvent in the formation of mesostructure for the zeolite with intact cell. As the molar ratio of Si to Al in the zeolite gel rose to 10, the obtained MT10 composite possessed three distinct diffraction peaks indexed as (100), (110), and (200) in the low-angle XRD patterns, implying the formation of ordered hexagonal mesoporous phase. Besides, MT10 exhibited the typical diffraction peaks of sodalite in wide-angle XRD pattern, and the peaks were broad because of the small size of the sodalite fragments. Formation of sodalite fragment in the MT10 led to the property different from that of AM10 with same aluminum content but synthesized by normal sol−gel method,[32] and the mesostructure of MT10 still maintained after it had been treated with boiling water for 12 h, while AM10 just possessed a broad (100) diffraction peak, and this peak almost disappeared after hydrothermal treatment because of the decline of the mesostructure of MCM-41 caused by incorporation large amount of aluminum[32,42] and the poor hydrothermal stability of normal Al-MCM-41.

Figure 2A illustrates the nitrogen adsorption−desorption isotherms of the MS samples synthesized by using different amount of TMB. Both MS3-4t-5b and MS3-6t-5b samples exhibited the isotherms similar to type IV with a large hysteresis loop in the p/p_0 range of 0.4−1.0, mirroring their hierarchical structure (Figure 2B). Specially, MS3-4t-5b sample had small mesopores around 6 nm, middle mesopore of 15 nm, and relative large mesopore of about 23 nm (Figure 2B). Because of the use of small amount of TMB, the mesostructure of MS3-2t-5b sample was unobvious, and its surface area and pore volume were relatively small (Table 1). As the molar ratio

(40) Karlsson, A.; Stöcker, M.; Schmidt, R. *Microporous Mesoporous Mater.* **1999**, *27*, 181.
(41) Felsche, J.; Luger, S.; Baerlocher, C. *Zeolite* **1986**, *6*, 367.
(42) Lin, H. -P.; Mou, C. -Y. *Acc. Chem. Res.* **2002**, *35*, 927.

Table 1. Structural Parameters and the Adsorption Capability of Porous Materials

sample	Si/Al	silica source	S_{BET} ($m^2 \cdot g^{-1}$)	S_{micro} ($m^2 \cdot g^{-1}$)	V_p ($cm^3 \cdot g^{-1}$)	V_{micro} ($cm^3 \cdot g^{-1}$)	NH_3-TPD ($mmol \cdot g^{-1}$)	adsorbed NPYR ($mmol \cdot g^{-1}$)[a]
MS3-2t-5b	3.1	Na_2SiO_3	309	265	0.20	0.12		
MS3-4t-5b	2.7	Na_2SiO_3	578	332	0.71	0.15	1.59	0.96
MS3-6t-5b	2.7	Na_2SiO_3	329	304	0.31	0.15	1.09	0.66
MS3-4t-7b	2.8	Na_2SiO_3	490	280	0.63	0.13		
MS3	2.8	Na_2SiO_3	296	249	0.18	0.12	1.05	0.62
NaY	2.86		672	631	0.34	0.31	1.02	1.16
MT3-4t-5b	3.4	TEOS	287	0	0.29	0	0.57	0.50
MT10-4t-5b	10.6	TEOS	674	0	0.68	0		
MT10	10.7	TEOS	437	43	0.41	0.03	0.61	0.60
AM10	10	TEOS	870	0	0.96	0	0.50	0.86

[a] The accumulated amount of NPYR that passed through the sample was 1.40 $mmol \cdot g^{-1}$.

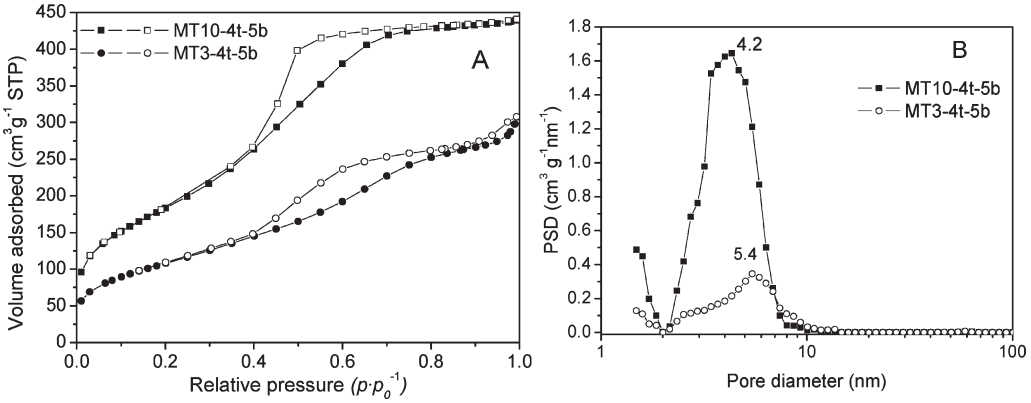

Figure 3. (A) Nitrogen adsorption−desorption isotherms and (B) pore distribution curves of MT samples.

of TMB/CTAB increased, the surface area and pore volume of MS3 composites first increased and then decreased, among them MS3-4t-5b exhibited the best mesostructure and largest mesopore volume (Table 1). On the other hand, All MS samples possessed a considerable number of micropore (Table 1), originating from the zeolite NaY fragments, for instance the micropore surface area of MS3-4t-5b sample was 57% of the total surface area. Figure 2C displays the nitrogen adsorption−desorption isotherms of MS3-4t-5b including the part at low relative pressure ($0 < p/p_0 < 0.01$). It showed a type I isotherm at p/p_0 between 0.0 and 0.3 that was the typical character of micropore material; as the relative pressure increase, the isotherms are type IV with type II behavior at the relative pressures close to unity, since the adsorption increases gradually and the isotherm does not show a distinct plateau at the relative pressures close to unity because of the broad mesopore distribution. Pore size distribution of the sample was evaluated from the adsorption isotherm by the density functional theory method, and as the result showed, the composite had the micropore size of 0.73 nm that was the characteristic window of NaY zeolite,[39] the peak of small mesopores around 5.8 nm, and the relatively broad and large mesopore with the maximum of 15 nm (Figure 2D). Different from the MS analogue, the MT3-4t-5b sample showed a different isotherm (a sharp step at $p/p_0 = 0.4$), and only one single pore distribution centered at 5.4 nm (Figure 3). Rather, the surface area of MT3-4t-5b was relatively small and no micropore was detected in the nitrogen sorption experiment (Table 1) because of the very small aperture of sodalite that could not adsorb N_2 molecule.[43]

Figure 4a displays the SEM images of MS3-4t-5b sample, which exhibits the relative uniform ribbed particles with the size about 500 nm, with the hierarchical pore on the nanocrystals' rough surface. Figure 4b illustrates the TEM image of MS3-4t-5b, in which both the hierarchical mesopores of 5 to 15 nm and the micropore of around 0.7 nm related to zeolite Y are visible. It was found that the zeolitic phase (marked with rectangle) was alternated with the mesoporous phase (marked with arrow area), indicating the presence of hierarchical mesoporous zeolite. On the other hand, MT3-4t-5b exhibited petal-like morphology (Figure 4c) with the satin surface, differing from that of Al-MCM-41; its TEM image showed a worm-like mesostructure (Figure 4d), and the zeolitic phase of sodalite could be observed in the high magnification image (the left of Figure 4d), further proving the crystallization of the aluminosilicate.

Figure 5A presents the ^{27}Al NMR spectra of aluminosilicates. Mesoporous AM3 sample exhibited an asymmetric spectrum containing a sharp peak at 52 ppm and a shoulder at 0 ppm, which were attributed to tetrahedral and octahedral Al of amorphous aluminosilicates,[44] respectively, since all of the mesostructured aluminosilicates

(43) Ríos, C. A.; Williams, C. D.; Fullen, M. A. *Appl. Clay Sci.* **2009**, *42*, 446.
(44) Wan, Y.; Ma, J. X.; Wang, Z.; Zhou, W. *Microporous Mesoporous Mater.* **2004**, *76*, 35.

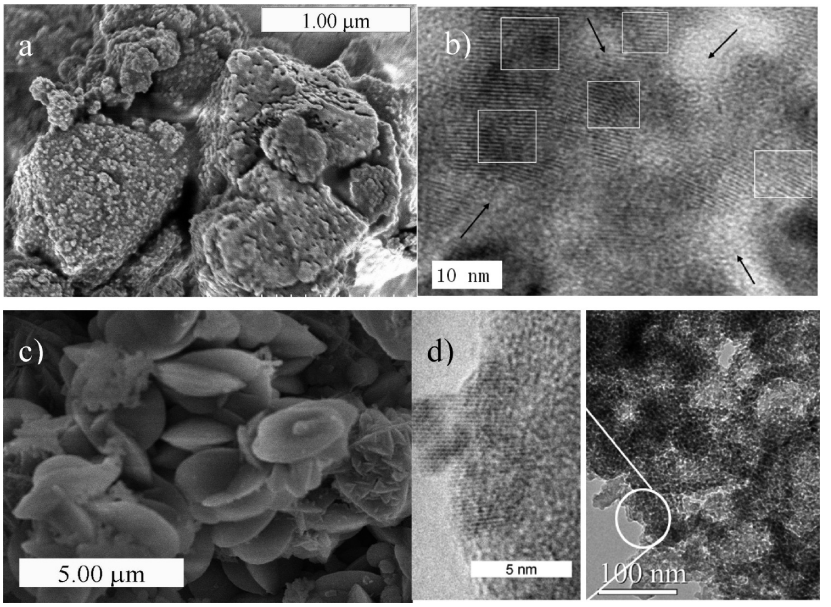

Figure 4. (a, c) SEM and (b, d) TEM images of MS3-4t-5b (a, b) and MT3-4t-5b samples (c, d).

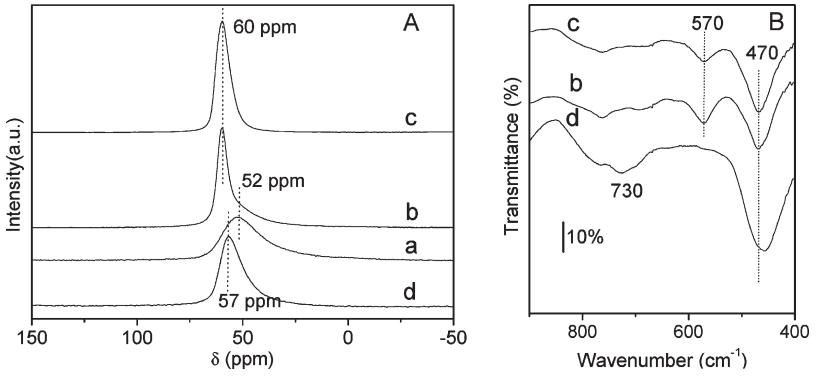

Figure 5. (A) ^{27}Al NMR and (B) IR spectra of (a) AM3, (b) mixture of NaY and AM3, (c) MS3-4t-5b, (d) MT3-4t-5b samples.

reported previously had the chemical shift in the range of 52 ± 2 ppm.[24] The spectrum of the mixture of zeolite Y with mesoporous AM3 was also asymmetric, possessing a sharp signal at 60 ppm with a shoulder at 52 ppm that originated form the tetrahedral Al in crystalline and amorphous aluminosilicates, respectively. However, the signal of aluminum shifted to 60 ppm in the spectrum of MS3-4t-5b sample, within the 59−65 ppm range observed for most zeolites,[45,46] indicating the presence of NaY fragments in the composite. Additionally, the spectrum of MS3-4t-5b was symmetric without the signal at 52 ppm, which implied the uniform chemical environment of aluminum in the sample. That is to say, the sample was relative pure phase. MT3-4t-5b sample exhibited a peak at 57 ppm in the ^{27}Al NMR spectrum (profile (d) Figure 5A). On the basis of the relationship between ^{27}Al chemical shift and the mean bond angle in framework aluminosilicates,[45] it is safe to infer that the mean Al−O−Si angle in MT3-4t-5b is substantially smaller (by ∼6°) than that in amorphous Al-MCM-41 because of the partial crystallization of the aluminosilicate.[24]

Figure 5B shows the IR spectra of the samples synthesized by assembling the zeolite gel of Si/Al = 3 with CTAB in the presence of TBA and TMB. When sodium silicate was used as the silica source, the obtained MS3-4t-5b sample exhibited two bands at 570 and 470 cm^{-1} on the IR spectra, attributing to double-ring of FAU zeolite and internal linkage vibrations of the TO_4 (T = Si or Al) tetrahedral,[39] respectively. For the sample MT3-4t-5b synthesized with TEOS as the silica source, both the bands at 730 and 460 cm^{-1} (originated from the overlap of the band at 470 cm^{-1} and 463 cm^{-1}) emerged, which indicated the presence of sodalite.[43]

The actual acidity of MS3-4t-5b composite was briefly examined by 2-propanol dehydration (Figure 6A). This sample showed the propene selectivity of 87% and 0.6% toward acetone at 250 °C, while the selectivity of propene rose to 99.5% and the conversion of 2-propanol to 100% at 280 °C, indicating the existence of some acid sites in the composite. It could convert half of the 2-propanol (52%)

(45) Lippma, E.; Samoson, A.; Mägi, M. *J. Am. Chem. Soc.* **1986**, *108*, 1730.
(46) Do, T. -O.; Nossov, A.; Springuel-Huet, M. -A.; Schneider, C.; Bretherton, J. L.; Fyfe, C. A.; Kaliaguine, S. *J. Am. Chem. Soc.* **2004**, *126*, 14324.

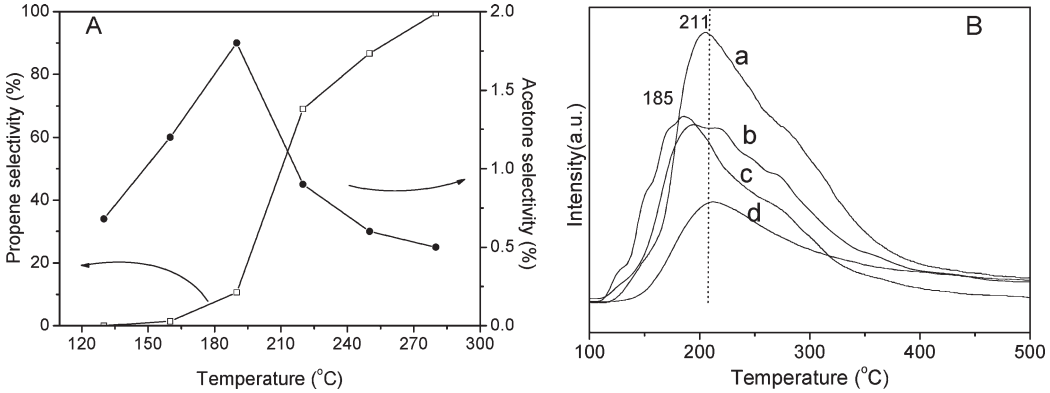

Figure 6. (A) Decomposition of 2-propanol over the sample of MS3-4t-5b. (B) NH_3-TPD spectra of (a) MS3-4t-5b, (b) MS3-6t-5b, (c) MT3-4t-5b, and (d) NaY samples.

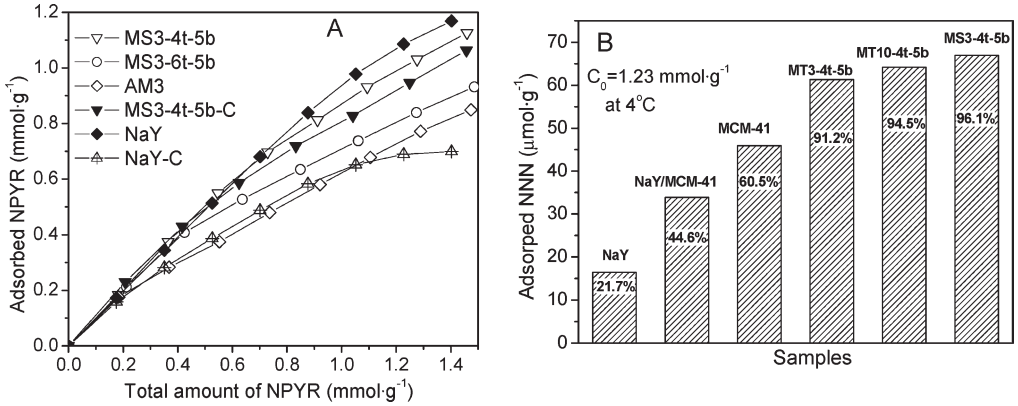

Figure 7. Adsorption of NPYR at 180 °C (A) and liquid adsorption of NNN at 4 °C (B) by porous materials.

at 200 °C, more than that by the Al-MCM-41(Si/Al = 15) (38%[47]) and NaY (3%, figure not shown), indicating the higher activity of MS3−4t-5b than that of NaY zeolite.

Both MS3-4t-5b and MS3-6t-5b samples had a desorption peak centered at 211 °C in the test of NH_3-TPD, while NaY zeolite showed a peak occurred at 185 °C (Figure 6B). Moreover, there was 1.59 mmol·g^{-1} of NH_3 desorbed from MS3-4t-5b, ~50% more than that from NaY (1.02 mmol·g^{-1}). On the other hand, the samples synthesized with sodium silica (MS3-4t-5b and MS3-6t-5b) desorbed more NH_3 than that prepared with TEOS (MT3-4t-5b), as demonstrated in Figure 6B.

Figure 7A displays the instantaneous adsorption of NPYR on the porous materials at 180 °C. In the case of 1.00 mmol·g^{-1} NPYR past through the adsorbent, about 62% of them were trapped by AM3, the Al containing MCM-41 with the Si/Al ratio of 3. Nonetheless, all of the samples synthesized by assembling the zeolite gel with the same Si/Al ratio exhibited a higher adsorptive capacity than AM3, and among them MS3-4t-5b could trap 89% of the NPYR. Zeolite NaY captured 94% of NPYR under the same conditions, and no doubt it was the best. However, coking treatment dramatically lowered the capacity of NaY from 94% to 63%, whereas MS-4t-5b only lost about one tenth of the activity (Figure 7A), owing to the excellent anti-coking of zeolitic mesoporous materials.

Figure 7B illustrates the liquid adsorption of NNN by the mesoporous composites and zeolite NaY at 4 °C to assess their actual performance on the adsorption of bulky nitrosamine. NaY zeolite trapped 22% of NNN in the solution because of its micropores, while MCM-41 adsorbed 60% because of its large pore size. Higher adsorptive ability was observed on the hierarchical porous materials, MT3-4t-5b and MT10-4t-5b adsorbed 91% and 95% of NNN in solution respectively while MS3-4t-5b could trap 96%. Under the same conditions, however, the mechanical mixture of NaY and MCM-41 with the weight ratio of 1:1 only adsorbed 45% of the NNN, which excludes the suspicion whether the MS3 sample is the mixture of zeolite and mesoporous silica.

4. Discussion

One aim of this study is to synthesize the hierarchical zeolite, such as the MS3-4t-5b sample that owns the relatively large mesopore to favor the transportation of mass and the active site to enhance the catalytic or adsorptive capability; especially, this hierarchical composite is expected to exhibit an excellent ability in capturing the carcinogen such as nitrosamines with various structures in environment. With the respect of trapping nitrosamines, zeolite NaY possesses the strong static force field

(47) Kanda, Y.; Kobayashi, T.; Uemichi, Y.; Namba, S.; Sugioka, M. *Appl. Catal., A* **2006**, *308*, 111.

toward the N-NO group of nitrosamines[38] and the excellent ability to adsorb volatile nitrosamine (Figure 7A), however, it is easily deactivated by coking due to the block of micropore therefore the adsorptive capacity decreased by one-third even when the 1.4% carbon deposited on it (Figure 7A). In addition, NaY could just trap 22% of the NNN in CH_2Cl_2 solution (Figure 7B), which is also caused by the geometric limitation of micropore. Thus, a new material with a high efficiency for trapping these carcinogens is desirable. It is true that introducing aluminum in the synthesis media of mesoporous silica samples can improve their activity in trapping the volatile nitrosamine such as NPYR, however, incorporation of too large quantity of aluminum often leads to the decline of their structure regularity.[32,42] Contrarily, through the precrystallization of the aluminosilicate, we could obtain the MT10 materials with a relatively ordered mesoporous structure and high alumina content as well as the improved hydrothermal stability (Figure 1D) because the SiO_4 and AlO_4 tetrahedron formed first during the precrystallization of aluminosilicate source in the presence of zeolite directing-agent, and the oligomer of tetrahedron and surfactant were further assembled toward ordered mesoporous structure. Since sodalite is the zeolite with 6-member ring window,[48] it could not adsorb the nitrogen with kinetic diameter of 0.36 nm therefore the microporous surface area of MT samples detected in nitrogen adsorption-desoprtion is quite small or zero (Table 1).

To get the mesoporous silica with zeolite Y fragment, sodium silica is employed as the silica source and the Si/Al ratio of gel is decreased to 3. The MS3 sample synthesized by assembling the zeolite gel only with the CTAB surfactant lacks the mesoporous structure (Low-angle XRD patterns not shown), but the MS3-4t-5b analogue synthesized with additive of TBA and TMB possesses both the characteristic of zeolite Y (profile (b) in Figure 1A) and a worm-like mesoporous structure (Figure 1B) which is also confirmed by the N_2 adsorption−desorption results (Figure 2C and 2D). It should be pointed out that in literature,[24−27] the zeolitic mesoporous materials can be obtained from the self-assembly of preformed zeolite nanoclusters with surfactants, but their XRD patterns show no diffraction peak of zeolite because the sizes of preformed zeolite nanoclusters are relatively small. Hence, it is still a challenge to obtain the mesoporous materials with relative intact zeolite framework, since the formation of an intact zeolite unit cell needs the preformed zeolite nanoclusters to grow to the relative large size, and this requirement will lead to the difficulty in the self-assembly between the large silica species and the nanoscale surfactants micelle, because the surfactants have a limited charge density that is not enough affinity to interact with the bulky silica species. Therefore, once the sample shows the typical diffraction peaks of zeolite, it would have no mesoporous structure, as aforementioned, in the absence of cosolvent and additive agent because the relative small surfactant micelle (2−3 nm) cannot enable the relative large zeolite nanoclusters to be assembled because of the deficient affinity.[30] Contrarily, in our research reported here, the synthesized MS3-4t-5b sample possesses a worm-like mesoporous structure and the characteristic peaks of zeolite Y once proper amount of the cosolvent and additive are used. TMB additive is widely applied in the synthesis of mesoporous materials as a swelling agent for the surfactant micelle in the aqueous solution.[49,50] The additive amount of TMB is crucial for the formation of mesostructure. As the ratio of TMB/CTAB was below 2, the surfactant micelles were not swollen owing to the preferential adsorption of low-substituted aromatic molecules near the quaternary ammonium headgroups due to cation−π interactions,[51] and the small micelles did not match to the zeolite fragments with relative large size, therefore the synthesized MS3-2t-5b had no mesostructure and thus possessed small pore volume (Figure 1C and Table 1). In the case that $4 <$ TMB/CTAB < 6, a considerable amount of TMB was solubilized in the core of micelles and swelled the CTAB micelles to mesoscale, which was facilitated by the more hydrophobic environment at the micellar interface given by the TMB interacted with the ammonium headgroups. As the TMB amount further increased, no additional TMB was incorporated into the micelles since the limited solubilization of TMB in CTAB micelles was reached and thus large amount of the TMB molecules remained out of the hydrophilic shell of the micelles to act as a barrier, preventing the interactions of these headgroups with silicate species. As the result, the obtained MS3−9t-5b sample exhibited no mesostructure (Figure 1C). However, mesoporous zeolites still could not be synthesized even when the surfactant micelles were swollen to the mesoscale because of the insufficient affinity between the micelles and the crystalline silicates species. Thereby, appropriate cosolvent TBA was added to solve this problem. For ionic amphiphilic surfactant, the repulsive interaction among the headgroups affects both the intra- and the inter- arrangement of micelle;[29] And addition of cosolvent can change the repulsion of the surfactants' headgroups and packing parameter, $g = V/la_0$, where V is the volume of the hydrophobic surfactant chains, l is the surfactant chain length, and a_0 is the effective area of the hydrophilic headgroup of the surfactant molecule at the interface.[42] In the present work, the TBA additive could reduce the repulsion of the hydrophilic headgroup and thus increased the g value, leading to the increased charge density of the micelle and enhancing the affinity between the micelles and the aluminosilica species. On the basis of these results mentioned above, the formation mechanism of mesoporous zeolite can be tentatively deduced as

(48) Khajavi, S.; Jansen, J. C.; Kapteijn, F. *J. Membr. Sci.* **2009**, *326*, 153.
(49) Boissière, C.; Martines, M. A. U.; Tokumoto, M.; Larbot, A.; Prouzet, E. *Chem. Mater.* **2003**, *15*, 509.
(50) Jiang, D. M.; Gao, J. S.; Li, J.; Yang, Q. H.; Li, C. *Microporous Mesoporous Mater.* **2008**, *113*, 385.
(51) Lefèvre, B.; Galarneau, A.; Iapichella, J.; Petitto, C.; Di Renzo, F.; Fajula, F. *Chem. Mater.* **2005**, *17*, 601.

Scheme 1. Proposed Route for the Synthesis of Hierarchical Mesoporous Zeolite

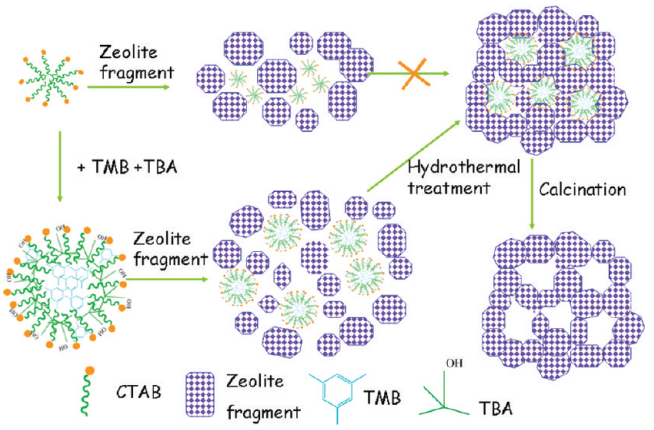

follows: TMB can swell the surfactant micelles to mesoscale, enabling the surfactant micelle to match with the relative large zeolite nanoclusters; meanwhile the incorporation of cosolvent TBA increases the charge density of the micelle surface and promotes zeolite nanocluster to be condensed and assemblyed on the surface of the micelle. Therefore, assembling the zeolite fragments in the presence of *tert*-butyl alcohol (TBA) and TMB can form the hierarchical mesoporous zeolite (Figure 3C and D). Scheme 1 proposed the possible route for the synthesis of hierarchical mesoporous zeolite. Zeolite fragment will not assemble on the normal CTAB surfactant micelle, due to the extreme small size of the micelle compared with that of zeolite fragment and the insufficient affinity of the micelle toward the zeolite fragment. When the TMB and TBA were added into the CTAB solution, the size of the micelle was enlarged while the charge density of the surfactant micelle was increased. Therefore, the strengthened interaction between the mesoscale micelle and the zeolite fragment promotes the formation of the hierarchical mesoporous structure in the presence of TMB and TBA. As expected, the resulting MS3-4t-5b sample shows the excellent ability in adsorption of NH_3 (1.59 $mmol \cdot g^{-1}$) and NPYR (0.96 $mmol \cdot g^{-1}$) as well as NNN (96%) along with the high ability to anti-coke, due to the increased accessibility of the adsorptive site in the zeolite thanks to the presence of mesopore that enhances the mass transport efficiency. Moreover, the potential use of cosolvent and swell agent TMB provides a clue to synthesize the mesoporous silica with hierarchical structure, affording the efficient adsorbent to capture the carcinogenic pollutants with various structures in the environment.

5. Conclusion

Mesoporous silica containing sodalite unit could be synthesized by assembling the precrystallized aluminosilicate with the cationic surfactant CTAB, which exhibited an improved hydrothermal stability and showed an excellent ability in capturing the volatile nitrosamines in airflow and the bulky tobacco specific nitrosamines in solution.

The hierarchical mesoporous zeolite Y was fabricated through the elaborate design of the mesoscale surfactant micelle with relative high charge intensity by adding TMB and cosolvent, which enabled the nanosized zeolite fragment to deposit and assemble on the micelle.

The presence of mesopore in the hierarchical composite made it to exhibit a better resistance to coking than zeolite NaY, and improved its adsorptive ability toward volatile nitrosamines such as NPYR. Especially, MT10 sample showed a capacity comparable to zeolite NaY for trapping NPYR in airflow and four time superior to NaY for adsorbing bulky NNN in solution.

Acknowledgment. Financial support from Grant 2008-AA06Z327 from the 863 Program of MOST, NSF of China (20773601, 20873059, and 20871067), Jiangsu Provincial Natural Science Foundation Industrial Supporting Program (BE2008126), Jiangsu Province Environmental Protection Bureau Scientific Research Program (2008005), and Analysis Centre of Nanjing University is gratefully acknowledged. The authors thank Mr. H.Y. Zhu (University of Wisconsin-Madison, USA) for his assistances.

Supporting Information Available: Nitrogen adsorption−desorption isotherm of MS3-4t-7b sample. This material is available free of charge via the Internet at http://pubs.acs.org.